Formation and Dissociation Kinetics of Nickel(II) with Ionophore A23187 in 80% Methanol–Water

Timothy P. Thomas,[1a] Douglas R. Pfeiffer,[1b] and Richard W. Taylor*[1a]

Contribution from the Department of Chemistry, University of Oklahoma, Norman, Oklahoma 73019, and The Hormel Institute, University of Minnesota, Austin, Minnesota 55912. *Received April 27, 1987*

Abstract: The formation and dissociation rate constants of the nickel(II) complexes of ionophore A23187 in 80% methanol–water at 25 °C have been determined with use of the stopped-flow method by monitoring changes in the ultraviolet spectra of the reacting species. Formation kinetics of the 1:1 complex were studied in the pH* range 5.18–6.18, employing excess Ni^{2+} to ensure pseudo-first-order behavior. The data are consistent with a model involving parallel reactions of Ni^{2+} with the anionic (A^-) and protonated (HA) forms of the ionophore, with the rate law being $d[NiA^+]/dt = (k_{Ni}^{A}[A^-] + k_{Ni}^{HA}[HA])[Ni^{2+}]$. The rate constants for the anionic form of A23187, k_{Ni}^{A}, and the protonated form, k_{Ni}^{HA}, are 1.8×10^6 and $\sim 400\ M^{-1}\ s^{-1}$, respectively. The value obtained for k_{Ni}^{A} is close to that predicted for the Eigen dissociative model, $k_f = K_{os}k^{M-S}$, where K_{os} and k^{M-S} are the outer-sphere equilibrium constant and metal–solvent exchange rate constant, respectively. The rate-determining step is proposed to be first-bond formation involving the carboxylate oxygen atom of the anionic form of the ionophore. The relatively low value of k_{Ni}^{HA} may indicate a shift of the rate-determining step to ring closure or could indicate a low population of the reactive form of the protonated ionophore, i.e., proton on the nitrogen of the *N*-methyl group. The dissociation kinetics of the 1:2 and 1:1 Ni^{2+}–A23187 complexes were studied by mixing the preformed complex with a large excess of H^+. The observed rate constant displayed saturation behavior with respect to $[H^+]$; $k_{obsd} = (k_d + k_H K_{NiAH}[H^+])/(1 + K_{NiAH}[H^+])$, where k_d and k_H are the dissociation rate constants of NiA^+ and $NiAH^{2+}$, respectively, and K_{NiAH} is the equilibrium constant for the reaction $NiA^+ + H^+ \rightleftarrows NiAH^{2+}$. With the NiA_2 complex, an initial absorbance jump was noted, corresponding to the reaction $H^+ + NiA_2 \rightarrow NiA + HA$. At a given $[H^+]$, the values of k_{obsd} were the same for both the 1:1 and 1:2 complexes. The values obtained for the parameters are $k_d = 0.048\ s^{-1}$, $k_H = 0.4\ s^{-1}$, and $K_{NiAH} = 880\ M^{-1}$. The value of log K_{NiA} derived from the ratio k_{Ni}^{A} to k_d (7.55) is in excellent agreement with the value obtained previously by fluorimetric titration (7.54).

The acyclic polyether carboxylic acid antibiotic A23187 (see Figure 1 for structure) facilitates the transport of divalent cations across naturally occurring and artificial membranes.[2,3] Ionophore A23187 is particularly noteworthy because of its high transport selectivity for divalent cations relative to monovalent cations[2,4] and has found widespread use as a tool to manipulate Ca^{2+} ion concentration gradients in a wide variety of biological membrane systems.[5] In order to better understand the transport properties of carboxylic acid ionophores in general and of A23187 in particular, we are studying the individual reactions that compose the overall process of ionophore-catalyzed cation transport.[6] The reactions that comprise the model are shown schematically in Figure 1. Determination of equilibrium and rate constant values for the various component steps of the overall cycle is a necessary prerequisite to the testing of this model and to gaining insight into the relationship between ionophore structure and transport selectivity. Values have been reported for the protonation and complex formation constants of A23187 with monovalent and divalent cations in homogeneous solution,[7-12] in two-phase extractions,[4] and in the presence of phospholipid vesicles.[13-15]

However, kinetic studies involving metal ion–A23187 complexes are scarce. Krause et al.[16] have reported the formation and dissociation rate constants for Mg^{2+}- and Ca^{2+}–A23187 complexes in methanol. Pfeiffer et al.[6] reported results of a preliminary kinetic study of Ni^{2+}–A23187 in 65% methanol–water, and Kolber and Haynes[15] have studied the transport kinetics of alkaline-earth cation–A23187 complexes in phospholipid membranes.

The present communication reports results of a detailed kinetic study of the formation and dissociation reactions of Ni^{2+} with A23187 in 80% methanol–water. The reactions of interest are given in eq 1 and 2, where A_T represents the protonated (HA)

$$Ni^{2+} + A_T \underset{k_d}{\overset{k_f}{\rightleftarrows}} NiA^+ \qquad (1)$$

$$NiA_x^{2-x} + H^+(\text{excess}) \rightarrow xHA + Ni^{2+} \qquad x = 1, 2 \qquad (2)$$

and anionic (A^-) forms of A23187. Ni^{2+} was chosen as the cation since the relatively slow solvent-exchange rate allows the reactions to be studied by stopped-flow technique.[6,17,18] Furthermore, a large body of kinetic data for Ni^{2+}–ligand complexation reactions is available for comparison.[19]

Materials and Methods

Nickel perchlorate was prepared by the reaction of ultrapure $NiCO_3$ (Aldrich, Milwaukee, WI) with a slight excess of $HClO_4$ (Fisher Scientific, Pittsburgh, PA), followed by recrystallization from hot water. The stock $Ni(ClO_4)_2$ solution was standardized by titration with EDTA.[20]

(1) (a) University of Oklahoma. (b) University of Minnesota.
(2) Reed, P. W.; Lardy, H. A. *J. Biol. Chem.* **1972**, *247*, 6970–6977.
(3) Taylor, R. W.; Kauffman, R. F.; Pfeiffer, D. R. In *The Polyether Antibiotics: Naturally Occuring Acid Ionophores*; Westley, J. W., Ed.; Dekker: New York, 1982; Vol. 1, pp 103–184.
(4) Pfeiffer, D. R.; Lardy, H. A. *Biochemistry* **1976**, *15*, 935–943.
(5) Reed, P. W. In *The Polyether Antibiotics: Naturally Occurring Acid Ionophores*; Westley, J. W., Ed.; Dekker: New York, 1982; Vol. 1, pp 185–302.
(6) Pfeiffer, D. R.; Taylor, R. W.; Lardy, H. A. *Ann. N.Y. Acad. Sci.* **1978**, *307*, 402–423.
(7) Kauffman, R. F.; Taylor, R. W.; Pfeiffer, D. R. *Biochemistry* **1982**, *21*, 2426–2435.
(8) Tissier, C.; Julliard, J.; Dupin, M.; Jeminet, G. *J. Chim. Phys. Phys.-Chim. Biol.* **1979**, *76*, 611–617.
(9) Albin, M.; Cader, B. M.; Horrocks, W. DeW., Jr. *Inorg. Chem.* **1984**, *23*, 3045–3050.
(10) Tissier, C.; Juillard, J.; Boyd, D. W.; Albrecht-Gary, A. M. *J. Chim. Phys. Phys.-Chim. Biol.* **1985**, *82*, 899–906.
(11) Chapman, C. J.; Puri, A. K.; Taylor, R. W.; Pfeiffer, D. R. *Biochemistry* **1987**, *26*, 5009–5018.
(12) Bolte, J.; DeMuynck, C.; Jeminet, G.; Juillard, J.; Tissier, C. *Can. J. Chem.* **1983**, *60*, 981–989.
(13) Kauffman, R. F.; Chapman, C. J.; Pfeiffer, D. R. *Biochemistry* **1983**, 22, 3985–3992.
(14) Taylor, R. W.; Chapman, C. J.; Pfeiffer, D. R. *Biochemistry* **1985**, *24*, 4852–4859.
(15) Kolber, M. A.; Haynes, D. H. *Biophys. J.* **1981**, *36*, 369–391.
(16) Krause, G.; Grell, E.; Albrecht-Gary, A. M.; Boyd, D. W.; Schwing, J. P. In *Physical Chemistry of Transmembrane Ion Motions*; Spach, G., Ed.; Elsevier: Amsterdam, 1983; pp 255–263.
(17) Garcia-Rosas, J.; Schneider, H. *Inorg. Chim. Acta* **1983**, *70*, 183–187.
(18) Pearson, R. G.; Ellgen, P. *Inorg. Chem.* **1967**, *6*, 1379–1384.
(19) Margerum, D. W.; Cayley, G. R.; Weatherburn, D. C.; Pagenkopf, G. K. (1978) In *Coordination Chemistry*; Martell, A. E., Ed.; ACS Monograph 174; American Chemical Society: Washington, DC, 1978; Vol. 2, pp 1–20.
(20) Vogel, A. I. In *Quantitative Inorganic Analysis*, 3rd ed.; Wiley: New York, 1961; p 435.

0002-7863/87/1509-6670$01.50/0

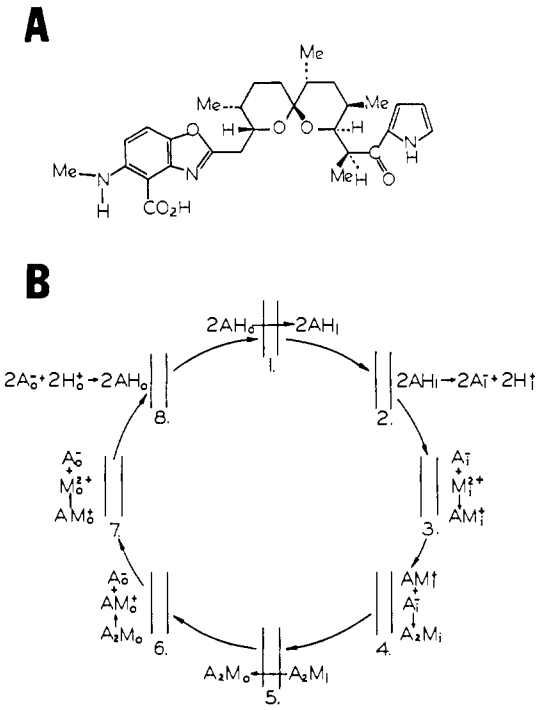

Figure 1. Structure and transport reaction of ionophore A23187. (A) Structure of the ionophore as originally reported by Chaney et al.[49] (B) Minimum number of sequential component reactions required to complete one cycle of divalent cation transport by A23187. The pairs of vertical lines shown in each step of the cycle are meant to illustrate the phospholipid bilayer membrane across which transport is occurring. The subscripts i and o associated with the various chemical species refer to location as inside or outside of the membrane, respectively.

Stock solutions of $HClO_4$ were prepared from the concentrated acid and standardized by titration with NaOH (J. T. Baker, Phillipsburg, NJ). Reagent-grade tetraethylammonium perchlorate, Et_4NClO_4 (Eastman Chemicals, Rochester, NY), tetraethylammonium hydroxide, Et_4NOH (Aldrich), primary standard Na_2H_2EDTA (Aldrich, gold label), and Mes, Ches, and Hepes buffers (Sigma Chemical, St. Louis, MO) were used as provided. The free acid of A23187 was obtained from Calbiochem (San Diego, CA). All glassware was acid-washed (sulfuric:nitric = 3:1, v/v).

Methanol–Water Solvents. Methanol–water solutions (80%, w/w) were prepared gravimetrically from distilled reagent-grade methanol (Fisher Scientific) and doubly distilled water. Measurements of pH* in methanol–water mixtures were carried out with use of a glass electrode (Beckman 41263) and a double-junction reference electrode (Corning 476067) with the outer chamber filled with 1.0 M KNO_3. The electrodes and pH meter (Orion 601) were calibrated with aqueous standard buffers (Fisher Scientific, Gram Pac) prior to equilibration with the methanol–water solvent. The operational pH* scales developed by de Ligny et al.[21,22] and Gelsema et al.[23,24] were then utilized to determine the value of pH*. The term pH* is defined as $-\log a_H^*$, where a_H^* is the activity of H^+ in the mixed solvent. The term pH*, when used in reference to the methanol–water mixture, has the same meaning as the term pH, when used in reference to an aqueous solution (see Rorabacher et al.[25] and references cited therein).

Spectral and Kinetic Measurements. Absorbance spectra were recorded on a Hitachi 100-80 or Cary Model 118 double-beam spectrophotometer equipped with a thermostated cell holder. All reactions were rapid and were studied by using a Durrum-Dionex stopped-flow system interfaced to a Cromemco Z2-D computer. The temperature of the reactants and the observation cell was maintained at 25.0 ± 0.1 °C with a circulating constant-temperature bath. The formation rates (eq 1) were

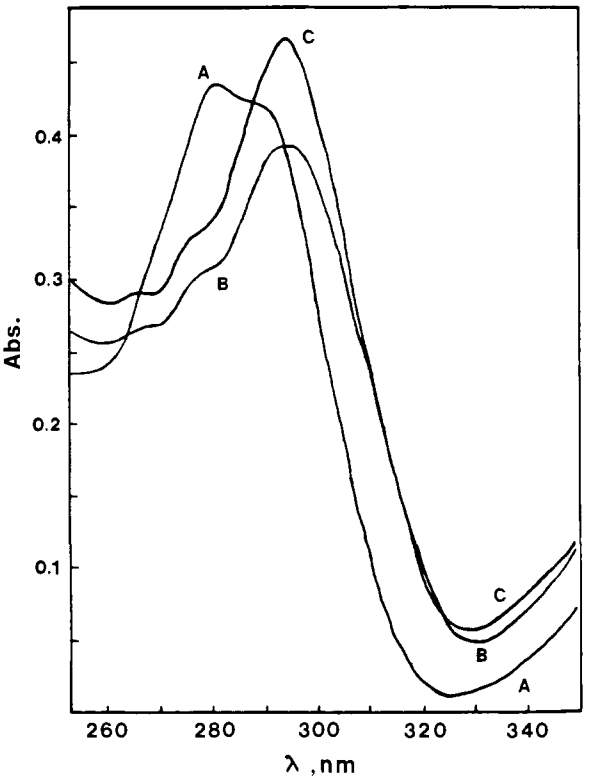

Figure 2. Absorbance spectra of A23187 with selected values of $[Ni^{2+}]$ at pH* 6.00. Spectra were obtained at 25.0 °C in 80% methanol–water containing 33 mM Et_4NClO_4 and 5 mM each of Mes, Hepes, and Ches buffers. The pH* of the solution was adjusted with Et_4NOH or $HClO_4$ and measured by procedures described in Materials and Methods. Key: $[A23187]_{TOT}$ = 25 μM; A, $[Ni^{2+}]$ = 0.0; B, $[Ni^{2+}]$ = 13.0 μM; C, $[Ni^{2+}]$ = 0.378 mM; path length 1 cm.

measured in the pH* range 5.18–6.18. The reaction progress was monitored at 310 nm. The reactions were carried out employing at least a 20-fold excess of Ni^{2+} to ensure pseudo-first-order conditions. These conditions also minimized formation of the NiA_2 species. At each pH* value, the reactions were initiated by mixing a solution of the ionophore (40–50 μM $A23187_{TOT}$, 5 mM Hepes, 5 mM Mes, and Et_4NClO_4) with an equal volume of a solution of the metal ion (1.0–5.0 mM Ni^{2+}, 5.0 mM Hepes, 5.0 mM Mes, and Et_4NClO_4). The ionic strength of each solution was maintained at μ = 0.050 ± 0.001 by adding the appropriate amount of Et_4NClO_4. The pH* values of the metal ion and ionophore solutions were adjusted to the desired value just prior to reaction with use of $HClO_4$ or tetraethylammonium hydroxide. The rates of the acid-assisted dissociation of the NiA^+ and NiA_2 complexes (eq 2) were studied by mixing equal volumes of an $HClO_4$ solution (0.76–37.9 mM H^+) with a solution of the Ni^{2+} complex. Solutions of the 1:2 NiA_2 complex were prepared with an excess of ionophore (20 μM Ni^{2+}, 40–50 μM A23187) while solutions of the 1:1 complex were prepared with a large excess of Ni^{2+} (2.0 mM Ni^{2+}, 50 μM A23187). The ionic strength of the solutions was maintained at 0.050 with use of Et_4NClO_4 as the supporting electrolyte. The pH* of the metal ion–ionophore solutions was adjusted to 6.5 ± 0.1 immediately before each experiment with $HClO_4$ or Et_4NOH. The reactions of the 1:1 complex were monitored at 311 nm while the reactions of the 1:2 complex were monitored at 311 nm and, in some cases, also at 285–286 nm. All concentrations given above refer to the values before mixing. At each set of reaction conditions, six to eight replicate runs were recorded.

All observed reactions obeyed first-order kinetics. The value of the observed rate constant, k_{obsd}, was obtained by least-squares analysis of eq 3, where Abs_i, Abs_0, and Abs_∞ are the instantaneous, initial, and final

$$\ln [Abs_i - Abs_\infty] = \ln [Abs_0 - Abs_\infty] - k_{obsd}t \qquad (3)$$

values of the absorbance, respectively, and t is the time in seconds. The value of absorbance used for Abs_∞ was the average of 50 points taken at least 8 half-lives after the reaction had been initiated (i.e., >99.7% completion).

Results

Formation Rate of NiA^+. The formation rates were studied by using a large excess of nickel ion to ensure pseudo-first-order

(21) de Ligny, C. L.; Luykx, P. F. M.; Rehbach, M.; Weineke, A. A. *Recl. Trav. Chim. Pays-Bas* **1960**, *79*, 699–712.
(22) de Ligny, C. L.; Luykx, P. F. M.; Rehbach, M.; Weineke, A. A. *Recl. Trav. Chim. Pays-Bas* **1960**, *79*, 713–726.
(23) Gelsema, W. J.; de Ligny, C. L.; Remijnse, A. G.; Blijleven, H. A. *Recl. Trav. Chim. Pays-Bas* **1966**, *85*, 647–660.
(24) Gelsema, W. J.; de Ligny, C. L.; Blijleven, H. A. *Recl. Trav. Chim. Pays-Bas* **1967**, *86*, 852–864.
(25) Rorabacher, D. B.; Mackellar, W. J.; Shu, F. R.; Bonavita, S. M. *Anal. Chem.* **1971**, *43*, 561–573.

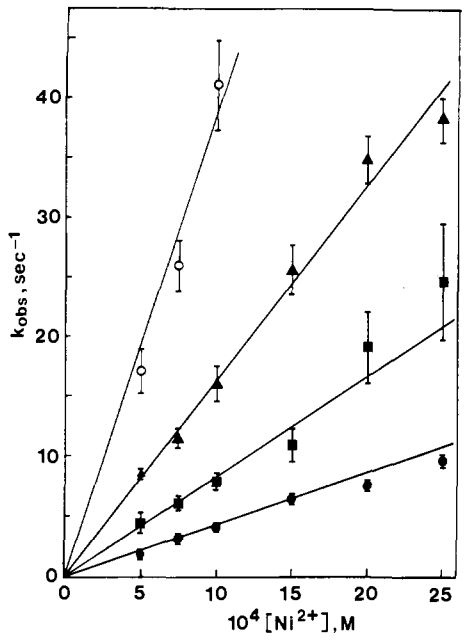

Figure 3. Effect of $[Ni^{2+}]$ and pH* on the formation kinetics of NiA^+. Plots of the pseudo-first-order rate constant, k_{obsd}, vs. $[Ni^{2+}]$ are shown for selected values of pH*. The concentration values shown refer to those after mixing. Reactant solutions were prepared as described in Materials and Methods. The error bars represent 1 standard deviation for the mean of six to eight replicate experiments. The calculated (solid) lines were obtained by using the resolved rate constants listed in Table III and eq 10. Key: closed circles, pH* 5.18; squares, pH* 5.48; triangles, pH* 5.78; open circles, pH* 6.18.

conditions and to minimize formation of the NiA_2 complex. Calculations using the program COMICS[26] with the equilibrium constant values listed in Table III indicate that less than 10% of the total ionophore concentration is present as NiA_2 under the conditions employed in these studies. All reactions obeyed first-order kinetics, and the value of k_{obsd} displayed a linear dependence on the excess nickel ion concentration. Figure 3 shows plots of the observed rate constant, k_{obsd}, as a function of $[Ni^{2+}]$ at several values of pH*. In the presence of a large excess of Ni^{2+}, eq 1 reduces to a pseudo-first-order reaction in the forward direction and a first-order reaction in the reverse direction. At a given nickel ion concentration, k_{obsd} is the sum of the first-order rate constants for the formation and dissociation reactions,[27] as in eq 4, where $[A]_{TOT}$ is the total concentration of uncomplexed

$$-\left[\frac{1}{[A]_{TOT}-[A]_{eq}}\right]\frac{d[A]_{TOT}}{dt} = k_{obsd} = k_f' + k_d = k_f[Ni^{2}] + k_d \quad (4)$$

ionophore ($[A^-] + [HA]$) at time t and $[A]_{eq}$ is the total concentration of uncomplexed ionophore when the reaction has reached equilibrium; i.e., $t \geq 8t_{1/2}$. Inspection of Figure 3 indicates that the formation rate constant, k_f, increases as the value of pH* increases. In the pH* range employed, A23187 exists as a mixture of the monoprotonated and anionic species. Since A23187 is a tridentate ligand,[28-30] it is possible for either one or both forms to react with Ni^{2+}. Since the protonation reactions of the ionophore are fast relative to the complexation reactions,[16] the overall

Table I. Observed Rate Constants for Formation Reactions of Ni^{2+} with A23187 in 80% Methanol–Water[a]

pH*	$10^4[Ni^{2+}]$,[b] M	k_{obsd},[c] s^{-1}	k_{calcd},[d] s^{-1}
5.18	5.0	1.7 ± 0.3	2.1
	7.5	3.2 ± 0.2	3.3
	10.0	4.1 ± 0.4	4.4
	15.0	6.4 ± 0.3	6.6
	20.0	7.6 ± 0.2	8.7
	25.0	9.7 ± 0.4	10.9
5.48	5.0	4.4 ± 0.9	4.1
	7.5	6.0 ± 0.6	6.2
	10.0	8.2 ± 0.7	8.3
	15.0	10.9 ± 1.3	12.5
	20.0	19.1 ± 3.0	16.6
	25.0	24.7 ± 4.9	20.8
5.63	10.0	9.4 ± 0.8	11.6
5.78	5.0	8.5 ± 0.3	8.1
	7.5	11.5 ± 0.7	12.1
	10.0	16.0 ± 1.4	16.1
	15.0	25.6 ± 2.1	24.1
	20.0	34.8 ± 1.9	32.2
	25.0	38.2 ± 1.9	40.2
6.18	5.0	17.0 ± 1.8	19.5
	7.5	25.8 ± 2.1	29.5
	10.0	41.0 ± 3.8	39.3

[a] For 25.0 °C, $[A23187]_{TOT}$ = 20–25 μM after mixing, where μ = 0.050. [b] Concentration after mixing. [c] Uncertainty expressed as 1 standard deviation of the mean value. [d] Values calculated by using eq 10 and rate constants listed in Table III.

formation reaction can be considered as the sum of parallel reactions of Ni^{2+} with A^- and HA, as shown in eq 5 and 6. The

$$H^+ + A^- + Ni^{2+} \xrightarrow{k_{Ni}^{A}} NiA^+ + H^+ \quad (5)$$

$$HA + Ni^{2+} \xrightarrow{k_{Ni}^{HA}} NiA^+ + H^+ \quad (6)$$

(K_{H1})

rate law for this system is given by eq 7. Combination of eq 7

$$d[NiA^+]/dt = k_f'[A]_{TOT} = (k_{Ni}^{A}[A^-] + k_{Ni}^{HA}[HA])[Ni^{2+}] \quad (7)$$

with the equilibrium expression $K_{H1} = [HA]/[A^-]a_H^*$ and the mass balance expression $[A]_{TOT} = [A^-] + [HA]$ gives eq 8, where

$$k_f = (k_{Ni}^{A} + k_{Ni}^{HA}K_{H1}a_H^*)/(1 + K_{H1}a_H^*) \quad (8)$$

a_H^* is the hydrogen ion activity, 10^{-pH^*}. Combining eq 4 and 8 followed by rearrangement gives eq 9. The values of k_d obtained

$$\frac{k_{obsd} - k_d}{[Ni^{+2}]}(1 + K_{H1}a_H^*) = k_{Ni}^{A} + k_{Ni}^{HA}K_{H1}a_H^* \quad (9)$$

from the plots in Figure 3 were within 1 standard deviation of the intercept; therefore, a value of $k_d = 0.048\ s^{-1}$, obtained from separate experiments (vide infra), was used in the calculations. Least-squares analysis of the left-hand side of eq 9 vs. $K_{H1}a_H^*$ for all data points yields the following values of the rate constants: $k_{Ni}^{A} = (1.86 \pm 0.08) \times 10^6\ M^{-1}\ s^{-1}$ and $k_{Ni}^{HA} = (4 \pm 2) \times 10^2\ M^{-1}\ s^{-1}$. The experimental values of k_{obsd}, $[Ni^{2+}]$, and pH* are listed in Table I along with the calculated rate constants, k_{calcd}, which were obtained by using the resolved values of k_{Ni}^{A} and k_{Ni}^{HA} and eq 10.

$$k_{calcd} = \frac{k_{Ni}^{A} + k_{Ni}^{HA}K_{H1}a_H^*}{1 + K_{H1}a_H^*}[Ni^{2+}] + k_d \quad (10)$$

Dissociation Rates of NiA^+ and NiA_2 in Strong Acid. The dissociation kinetics of metal ion–ionophore complexes may be studied with use of excess hydrogen ion as a scavenger.[16,33] The overall reaction shown in eq 2 may be expanded to give the stepwise sequence in eq 11 and 12. Under reaction conditions

$$NiA^+ \rightleftarrows Ni^{2+} + A^- \qquad k_d,\ k_f \quad (11)$$

$$A^- + H^+ \rightarrow HA \text{ (or } H_2A^+) \qquad k_p \quad (12)$$

(26) Perrin, D. D.; Sayce, I. G. *Talanta* **1967**, *14*, 833–842.
(27) Frost, A. A.; Pearson, R. G. In *Kinetics and Mechanisms*, 2nd ed.; Wiley: New York, 1961; pp 186–187.
(28) Chaney, M. O.; Jones, N. D.; Debono, M. *J. Antibiot.* **1976**, *29*, 424–427.
(29) Smith, G. D.; Duax, W. L. *J. Am. Chem. Soc.* **1976**, *98*, 1578–1580.
(30) Deber, C. M.; Pfeiffer, D. R. *Biochemistry* **1976**, *15*, 132–141.
(31) Baker, E.; Maslen, E. N.; Watson, K. J.; White, A. H. *J. Am. Chem. Soc.* **1984**, *106*, 2860–2864.
(32) Alléaume, M.; Barrans, Y. *Can. J. Chem.* **1985**, *63*, 3482–3485.
(33) Cox, B. G.; Schneider, H. *J. Am. Chem. Soc.* **1977**, *99*, 2809–2811.

Table II. Rate Constants for the Dissociation of NiA^+ and NiA_2 Complexes in Strong Acid in 80% Methanol–Water[a]

	k_{obsd},[b] s^{-1}	
$[H^+]$,[c] mM	$[Ni^{2+}] = 10\ \mu M$[c]	$[Ni^{2+}] = 1.0$ mM[c]
0.38	0.142 ± 0.003	
0.57	0.151 ± 0.011	
0.76	0.189 ± 0.008	
1.14	0.225 ± 0.009	
1.52	0.250 ± 0.007	
2.28	0.273 ± 0.013	
3.03	0.314 ± 0.006	
3.79	0.314 ± 0.006	
5.31	0.320 ± 0.015	0.325 ± 0.041
8.34	0.365 ± 0.015	0.391 ± 0.043
11.38	0.380 ± 0.012	0.363 ± 0.052
15.17	0.369 ± 0.016	0.382 ± 0.010
18.96	0.365 ± 0.018	0.383 ± 0.022

[a] Temperature 25.0 °C, $\mu = 0.048 \pm 0.002$, $[A23187]_{TOT} = 25\ \mu M$ after mixing. [b] Uncertainty expressed as 1 standard deviation. [c] Concentrations given are those after mixing.

Table III. Equilibrium and Rate Constants of Ni^{2+}–A23187 Complexes in 80% Methanol–Water[a]

$\log K_{HI} = 7.85 \pm 0.05$[b]	$k_{Ni}^{A} = (1.8 \pm 0.3) \times 10^6\ M^{-1}\ s^{-1}$
$\log K_{NiA} = 7.54 \pm 0.06$[c]	$k_{Ni}^{HA} = (4 \pm 2) \times 10^2\ M^{-1}\ s^{-1}$
$\log K_{NiA_2} = 8.6$[d]	$k_d = 0.048 \pm 0.013\ s^{-1}$
$\log K_{NiAH} = 2.94 \pm 0.09$	$k_H = 0.40 \pm 0.04\ s^{-1}$

[a] For 25.0 °C, $\mu = 0.050$ M (Et_4NClO_4); uncertainties expressed as 1 standard deviation. [b] Reference 7. [c] Reference 11. [d] Reference 48.

where $k_p[H^+] \gg k_f[Ni^{2+}]$, A^- may be treated as a steady-state intermediate and the rate of HA formation, $d[HA]/dt$, is equal to $k_d[NiA]_{TOT}$, for the case where there is no dissociation pathway involving H^+ attack prior to or at the rate-determining step. The use of a large excess of Ni^{2+} ($[Ni^{2+}] = 1.0$ mM) gave reactant solutions with NiA^+ as the predominant complex species. Equilibrium species distribution calculations for these conditions indicated that the final $[H^+]$ (after mixing) must be greater than 5.0 mM in order to drive the overall dissociation reaction (eq 11 and 12) to completion. A single reaction trace was observed for reactions carried out under these conditions, and all reactions displayed pseudo-first-order kinetic behavior. The values of the observed rate constants are listed in Table II. Due to the large excess $[Ni^{2+}]$ required to produce NiA^+ as the predominant complex species, the useful range of $[H^+]$ was relatively narrow. A wider H^+ concentration range can be employed if NiA_2 is the major form of the complex. Under the conditions described in Materials and Methods ($[Ni^{2+}] = 10\ \mu M$, $[A23187] = 25\ \mu M$), the lower end of the $[H^+]$ range can be extended to 0.5 mM. When equal volumes of these reactant solutions were mixed, a single pseudo-first-order reaction trace was observed in the wavelength region 310–320 nm. Inspection of Figure 2 reveals that the NiA^+ and NiA^2 species have similar absorbance properties in this region. However, at shorter wavelengths (280–285 nm), the spectra of NiA_2, NiA^+, and HA are distinct from each other with $Abs(HA) > Abs(NiA^+) > Abs(NiA_2)$. Stopped-flow experiments monitored at 286.5 nm revealed an absorbance "jump" that occurred during the mixing time of the instrument (<3 ms), followed by a pseudo-first-order reaction trace. A typical example is shown in Figure 4. The relative values of the absorbance changes for the rapid "jump" and the observable reaction (~6:1) are essentially the same as those obtained from the spectra shown in Figure 2. The fast process most likely represents the rapid removal of one molecule of A^- from NiA_2 as shown in eq 13. The

$$NiA_2 + H^+ \rightleftarrows NiA^+ + HA \qquad (13)$$

equilibrium constant, K, for this reaction is given by eq 14. Using

$$K = K_{HI}/K_{NiA_2} = [NiA^+][HA]/[NiA_2][H^+] \qquad (14)$$

the values of K_{HI} and K_{NiA_2} listed in Table III gives $K \simeq 0.18$. For the reaction conditions $[Ni^{2+}] = 10\ \mu M$, $[A23187] = 25\ \mu M$, and $[H^+] = 1.0$ mM, ~93% of the NiA_2 is converted to NiA^+ and HA according to the reaction represented by eq 13. As the $[H^+]$ increases, the degree of conversion will also increase (8 mM H^+; $[NiA^+]/[Ni]_{TOT} = 0.99$). The observed rate constants display a saturation-type behavior with respect to $[H^+]$ as shown in Figure 5. The relationship between k_{obsd} and $[H^+]$ is given by eq 15.

$$k_{obsd} = (a + b[H^+])/(1 + c[H^+]) \qquad (15)$$

For comparable values of $[H^+]$, the values of k_{obsd} are the same, within experimental error, for reactions starting with NiA^+ or NiA_2 as the major complex species. The values of k_{obsd} are listed

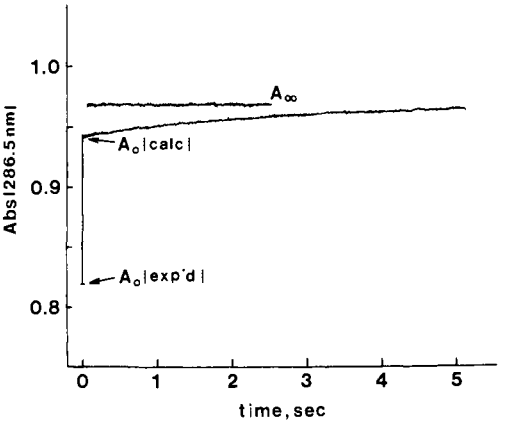

Figure 4. Acid-assisted dissociation of Ni^{2+}–A23187 complexes in 80% methanol–water at 25.0 °C. Stopped-flow absorbance vs. time trace at 286.5 nm of the reaction initiated by mixing a solution containing 50.0 μM A23187 and 20.0 μM Ni^{2+} at pH* 6.0 with an equal volume of a solution containing 6.07 mM H^+ (concentraton values prior to mixing). The other reactant solution constituents are as described in Materials and Methods. Under the conditions employed, the ionophore exists predominantly as the NiA_2 complex (~95%) before mixing with acid. The ordinate value labeled A_0(exp'd) was obtained by substitution of the measured absorbance values of the individual reactant solutions into the expression $A_0(exp'd) = [A_0(NiA_2) + A_0(HClO_4)]/2$. The ordinate value labeled A_0(calc) was obtained from the fit of the experimental reaction trace to eq 3.

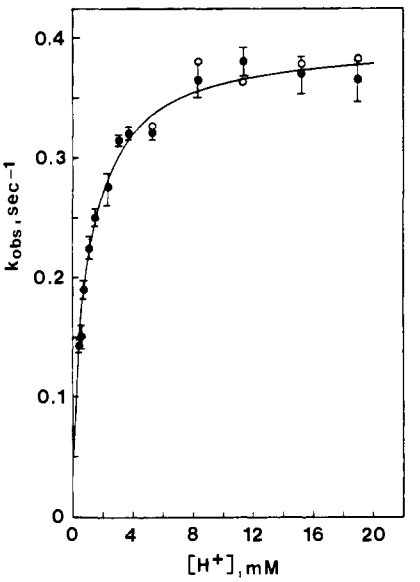

Figure 5. Effect of $[H^+]$ on the pseudo-first-order rate constants, k_{obsd}, for the dissociation of NiA^+ and NiA_2 in 80% methanol–water at 25.0 °C. Key: solid circles, $[A23187]_{TOT} = 25.0\ \mu M$, $[Ni^{2+}]_{TOT} = 10.0\ \mu M$; open circles, $[A23187]_{TOT} = 25.0\ \mu M$, $[Ni^{2+}]_{TOT} = 1.0$ mM; other components as described in Materials and Methods. The concentrations refer to the values after mixing. The error bars (solid circles) represent 1 standard deviation of the mean of six to eight replicate runs. The error bars of the open circles are omitted for clarity; however, the relative standard deviations of these runs are ≲±10%. The solid line was obtained by a nonlinear least-squares fit of all individual data points to eq 15.

in Table II. Nonlinear least-squares fit of all the data to eq 15 gives the following values for the parameters: $a = (4.8 \pm 1.3) \times 10^{-2}$, $b = (3.5 \pm 0.4) \times 10^{2}$, and $c = (8.8 \pm 0.9) \times 10^{2}$.

Discussion

Ionophore A23187 forms 1:2 metal ion–ligand complexes with a variety of cations.[3] Structural studies reveal that each ionophore molecule acts as a tridentate ligand, utilizing a carboxylate oxygen, the benzoxazole nitrogen, and the ketopyrrole carbonyl oxygen atoms as donor atoms.[28-32,34,35] These studies also have shown that the 1:2 complexes are stabilized by a network of intramolecular hydrogen bonds. When the appropriate reaction conditions are chosen, it is possible to have either NiA^+ or NiA_2 as the predominant complex species in solution.[11]

The kinetics of formation of the NiA^+ complex were studied by using a sufficient excess of the Ni^{2+} to ensure pseudo-first-order kinetics and to minimize formation of the NiA_2 complex. The ligand-substitution reactions of Ni^{2+} have been studied extensively in water[19] and to a lesser extent in other coordinating solvents.[36] In water and methanol, these reactions generally follow what is called a dissociative-interchange, or I_d, model.[37] According to this model, the rate of first-bond formation is governed by the rate of solvent exchange at the metal ion center. For many multidentate ligands, the formation of the first metal ion–ligand bond is the rate-determining step of the complexation reaction. The formation rate constant, k_f, may be predicted from the expression in eq 16, where K_{os} is the equilibrium constant for the

$$k_f = K_{os} k^{M\text{-}S} \tag{16}$$

formation of an outer-sphere complex and $k^{M\text{-}S}$ is the rate constant for metal ion–solvent bond rupture. The value of K_{os} is based on diffusion and may be calculated from the relationships given in eq 17–19, where N = Avogadro's number, a = distance of closest

$$K_{os} = [4/3\pi N a^3] \exp(-U(a)/k_B T) \times 10^{-3} \tag{17}$$

$$U(a) = \frac{Z_1 Z_2 e_0^2}{aD} - \frac{Z_1 Z_2 e_0^2 K}{D(1 + Ka)} \tag{18}$$

$$K = (8\pi N e_0^2 I / 1000 D k_B T)^{1/2} \tag{19}$$

approach, k_B = Boltzmann's constant, e_0 = charge of an electron, D = bulk dielectric constant, I = ionic strength, Z_1 and Z_2 = charges of reactants, and T = absolute temperature.[37,38] In 80% methanol–water, K_{os} values of 10 and 0.2 M^{-1} are calculated for Ni^{2+} reacting with A^- and HA, respectively. A value of $\sim 6 \times 10^4$ s^{-1} has been estimated for $k^{Ni\text{-}S}$ in 80% methanol–water.[39] This is somewhat larger than the analogous value in pure water (3.0×10^4 s^{-1}) determined by NMR methods.[36] In 80% methanol–water, the predominate solvated Ni^{2+} species is $Ni(H_2O)_5(CH_3OH)^{2+}$[40] and this species is thought to be more labile than $Ni(H_2O)_6^{2+}$ or $Ni(H_2O)_4(CH_3OH)_2^{2+}$.[41] Substitution of the appropriate values of K_{os} and $k^{Ni\text{-}S}$ into eq 16 gives k_{Ni}^{A}(calcd) $= 7 \times 10^5$ M^{-1} s^{-1} and k_{Ni}^{HA}(calcd) $= 1.2 \times 10^4$ M^{-1} s^{-1}. The experimental value of k_{Ni}^{A}, 1.8×10^6 M^{-1} s^{-1}, is in reasonable agreement with the value calculated by eq 16–19. Therefore, it appears that the formation kinetics of NiA^+ may be described by the dissociative interchange model. On the basis of electrostatic and steric considerations and the strengths of the potential donor atoms, it is likely that rate-determining first-bond formation involves the carboxylate oxygen atom and Ni^{2+}. First-bond formation involving the ketopyrrole carbonyl oxygen, a weaker donor

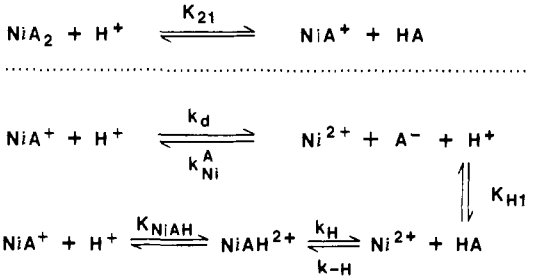

Figure 6. Reaction scheme for the formation and dissociation of Ni^{2+}–A23187 complexes in slightly acidic to strongly acidic 80% methanol–water. The protonation equilibria represented by K_{H1}, K_{21}, and K_{NiAH} are presumed to be rapid relative to the metal–ligand reactions.

atom, would require a fairly substantial ligand rearrangement to effect ring closure. In this situation, ring closure often becomes the rate-determining step and the formation rate constants are lower than the expected value.[19] For the case where the first bond is between Ni^{2+} and the carboxylate oxygen, the second step involves formation of a six-membered chelate ring with the benzoxazole nitrogen. The formation rate constants of several divalent cations with a related compound, the anionic form of 8-quinolinol, agree with the predicted values, indicating that ring closure is not the rate-limiting step.[42,43] Thus, the anionic form of A23187 most likely reacts by formation of a chelate involving the benzoxazole carboxylate oxygen and aromatic nitrogen, followed by coordination of the ketopyrrole carbonyl oxygen. Initial chelate formation labilizes the remaining inner-sphere solvent molecules,[19] which prevents the second ring closure, involving the carbonyl oxygen, from becoming the rate-determining step. The formation rate constants for the A23187 anion with Mg^{2+} in 100% methanol, 70% methanol–water,[16] and 65% methanol–water[6] also appear to agree with a mechanism involving first-bond formation as the rate-limiting step. A recent study of Lasalocid A with Ni^{2+} in methanol indicates that first-bond formation is the rate-determining step for the anonic form of that ionophore.[17]

The experimental value of k_{Ni}^{HA} is significantly lower ($\sim$40-fold) than the predicted value. This drastic reduction also supports the idea that the Ni^{2+}–carboxylate oxygen bond formation is the first step in complexation of the anion. The relatively low value of k_{Ni}^{HA} may be due to one or more of the following factors: rate-limiting proton transfer, ring closure, or a low population of a reactive species with the dissociable proton on the *N*-methylamino substituent of the benzoxazole moiety. Rate-limiting proton transfer has been ruled out as a cause for the abnormally low formation rate constants of molecular 8-quinolinol;[42,43] therefore, it is unlikely that this is also the cause for the low values of k_{Ni}^{HA}. Since ring closure does not appear to be rate limiting for the reactions of the anion, steric effects on closure are probably not important for the protonated ligand. However, if first-bond formation to Ni^{2+} involves the benzoxazole ring nitrogen, ring closure could become rate limiting due to the large dissociation rate of the weakly bound monodentate intermediate. On the other hand, the reactive form of HA may be a species with the proton on the nitrogen atom of the *N*-methylamino group adjacent to the carboxylate. Since the protonation of the carboxylate is favored,[7] the fraction of the protonated ionophore in the reactive form may be considerably less than unity.

The acid-induced dissociation of NiA^+ and NiA_2 exhibits a complex hydrogen ion dependence as shown in Figures 4 and 5. For initial reaction conditions where NiA_2 is the predominate complex species, a reaction characterized by an absorbance jump at 285–286 nm occurs in the mixing time of the stopped-flow instrument. The absence of a similar jump at 310–320 nm, where the spectra of NiA^+ and NiA_2 coincide, supports the idea that the initial rapid reaction corresponds to the conversion of NiA_2 to NiA^+ and HA (see eq 13). The observable reaction trace at 286.5 nm yields the same value of k_{obsd} as reactions monitored

(34) Anteunis, M. J. O. *Bioorg. Chem.* **1977**, *6*, 1–11.
(35) Pfeiffer, D. R.; Deber, C. M. *FEBS Lett.* **1979**, *105*, 360–364.
(36) Coetzee, J. F. *Pure Appl. Chem.* **1977**, *49*, 27–44.
(37) Wilkins, R. G. In *The Study of Kinetics and Mechanism of Reactions of Transition Metal Complexes*; Allyn & Bacon: Boston, 1974; p 183.
(38) Fuoss, R. M. *J. Am. Chem. Soc.* **1958**, *80*, 5059–5064.
(39) Jambor, L. G. Ph.D. Dissertation, Wayne State University, 1975.
(40) Rorabacher, D. B.; Shu, F. G.; Taylor, R. W.; Jambor, L. G.; Wheeler, L. H., submitted for publication in *Inorg. Chem.*
(41) Mackellar, W. J.; Rorabacher, D. B. *J. Am. Chem. Soc.* **1971**, *93*, 4379–4386.
(42) Hague, D. N.; Eigen, M. *Trans. Faraday Soc.* **1966**, *62*, 1236–1242.
(43) Johnson, W. A.; Wilkins, R. G. *Inorg. Chem.* **1970**, *9*, 1917–1921.

at 311 nm under the same conditions. Therefore, the observed reaction traces for the acid-induced dissociation of NiA^+ and NiA_2 correspond to the dissociation of the 1:1 complex. The saturation-type behavior with respect to $[H^+]$ is consistent with the reaction mechanism shown in Figure 6. Krause et al.[16] have proposed a similar scheme to explain the reactions of Ca^{2+} and Mg^{2+} complexes of A23187 in 100% methanol. With use of the notation of the scheme in Figure 6, eq 15 may be written as in eq 20. The dissociation process occurs via parallel uncatalyzed

$$k_{obsd} = (k_d + k_H K_{NiAH}[H^+])/(1 + K_{NiAH}[H^+]) \quad (20)$$

(k_d) and proton-assisted ($K_{NiAH}k_H$) pathways. The resolved rate constant and equilibrium constant values are listed in Table III. The value obtained for k_d, combined with the value of k_{Ni}^A, derived from the formation rate experiments, gives a calculated value 7.55 for log K_{NiA}. This is in excellent agreement with the value of 7.54 obtained by fluorometric titration techniques.[11] The k_d value for Ni^{2+} may be compared with the analogous value obtained for Mg^{2+} in 70% methanol–water, 89 s^{-1},[16] and a preliminary value of ~30 s^{-1} in 80% methanol–water.[44] The values of k_{Mg}^A are 3.8×10^5 M^{-1} s^{-1} in 70% methanol–water and $\sim 1 \times 10^6$ M^{-1} s^{-1} in 65% methanol–water.[6] Therefore, the complexation selectivity of $\sim 2 \times 10^3$ (K_{NiA}/K_{MgA}) for Ni^+ over Mg^{2+}[16] is reflected primarily in the difference in the respective k_d values. The acid-assisted dissociation pathway involves rapid formation of a protonated Ni^{2+}–A23187 complex, $NiAH^{2+}$, which then undergoes first-order dissociation to the products, Ni^{2+} and HA. Similar behavior was reported for the Ca^{2+} and Mg^{2+} complexes of A23187 in 100% methanol[16] and for the acid-induced dissociation of sodium monensin in ethanol.[45] Furthermore, evidence for complexes of protonated monesin with monovalent cations in solution[46] and in the solid state[47] has been reported. The overall equilibrium constant, K', for the bottom reaction shown in Figure 6 is equivalent to $K_{HI}\gamma_H/K_{NiA}$, where γ_H is the activity coefficient for H^+ in 80% methanol–water. With use of the relationships

$$K' = k_{NiA}^H/k_{Ni}^{HA} = K_{NiAH}k_H/k_{Ni}^{HA} \quad (21)$$

and $\gamma_H = 0.64$ and the values listed in Table III, a value of 270 M^{-1} s^{-1} is calculated for k_{Ni}^{HA}. This is in good agreement with the somewhat imprecise value of 400 M^{-1} s^{-1} obtained from analysis of the formation kinetics. The initial site of proton attack may be the benzoxazole *N*-methylamino nitrogen, since this group is not involved in metal ion coordination. The proximity of the protonated amino group to the carboxylate carbonyl oxygen would facilitate an intramolecular proton transfer, thus enhancing the rate of nickel–carboxylate oxygen bond rupture.

The following observations may be made with regard to the complexation–dissociation kinetics of A23187. A23187 forms 1:1 complexes via parallel reactions of the anionic and protonated forms of the ionophore with the metal ion. The anionic form is much more reactive than the protonated form of the ionophore. Dissociation of the 1:1 and 1:2 Ni^{2+}–A23187 complexes in acidic medium occurs via parallel uncatalyzed and proton-assisted pathways. At pH* values greater than ~5.5, the acid-assisted pathway is negligible relative to the uncatalyzed (k_d) pathway. However, the effect of general acids, HX (i.e., CH_3COOH) is not yet known. The rates of formation seem to parallel the known solvent exchange rates of the cation for Mg^{2+} and Ni^{2+}, but the situation is not clear for more labile cations like Ca^{2+}[16] and Zn^{2+}. The high affinity of A23187 for the first-row transition-metal cations[11] coupled with the potentially slow dissociation rates may effect the Ca^{2+} transport rates at low ionophore concentrations.

Acknowledgment. This work was supported in part by U.S. Public Health Service Grant GM-24701 from the National Institutes of Health and by the University of Oklahoma Research Council.

(44) Thomas, T. P.; Taylor, R. W., unpublished result.
(45) Cox, B. G.; Firman, P.; Schneider, H. *J. Am. Chem. Soc.* **1985**, *107*, 4297–4300.
(46) Hoogerheide, J. G.; Popov, A. I. *J. Solution Chem.* **1979**, *8*, 83–95.
(47) Ward, D. L.; Wei, K. T.; Hoogerheide, J. G.; Popov, A. I. *Acta Crystallogr., Sect. B: Struct. Crystallogr. Cryst. Chem.* **1978**, *B34*, 110–115.
(48) Chapman, C. J.; Pfeiffer, D. R., unpublished result.
(49) Chaney, M. O.; Demarco, P. B.; Jones, N. D.; Occolowitz, J. L. *J. Am. Chem. Soc.* **1974**, *96*, 1932–1933.

Experimental Electron Density Distribution of Naloxone Hydrochloride Dihydrate, a Potent Opiate Antagonist

Cheryl L. Klein,[1a] Richard J. Majeste,[1b] and Edwin D. Stevens*[1c]

Contribution from the Department of Chemistry, Xavier University of Louisiana, New Orleans, Louisiana 70125, the Department of Chemistry, Southern University at New Orleans, New Orleans, Louisiana 70126, and the Department of Chemistry, University of New Orleans, New Orleans, Louisiana 70148. *Received September 2, 1986*

Abstract: The electron density distribution of naloxone hydrochloride dihydrate has been determined from high-resolution single-crystal X-ray diffraction measurements at 90 K. Intensities of 21 509 reflections were measured with Mo Kα radiation to a resolution of $((\sin\theta)/\lambda)_{max} = 1.0$ Å^{-1}. Averaging symmetry-related reflections yielded a set of 8573 independent reflections with an internal agreement factor of 2.7%. Least-squares refinement with a conventional spherical atom model converged at $R = 3.3\%$ and $R_w = 4.3\%$. Refinement with a multipole expansion model including parameters describing valence electron deformations yielded $R = 2.7\%$ and $R_w = 3.7\%$. Maps of the experimental electron density distribution have been calculated by using model structure factors from the multipole refinement. Proper treatment of the X-ray phases increases covalent bond peak heights by ca. 50% compared with electron density maps based on spherical atom phases. The experimental electron deformation density shows well-resolved peaks in all covalent bonds and two nonbonding peaks on the carbonyl oxygen. Only a single peak is observed for the nonbonding electrons on the furan oxygen, hydroxyl oxygens, and water molecules. Net atomic charges, obtained from X-ray monopole populations, are in qualitative agreement with charges derived from theoretical calculations. The concept of "local area charges" is introduced to minimize partitioning effects on the atomic charges. The nitrogen atom is found to have a negative net atomic charge of −0.52, despite the formal positive charge.

X-ray structure determination has long been an extremely powerful tool in attempts to derive quantitative structure–activity relationships of drugs and other biologically significant molecules. Accurate low-temperature X-ray measurements may be used,

0002-7863/87/1509-6675$01.50/0